Probing spatial variations in the index of refraction of air: a simple experiment using shadowgraph techniques

2001 Eur. J. Phys. 22 541

(http://iopscience.iop.org/0143-0807/22/5/311)

INSTITUTE OF PHYSICS PUBLISHING EUROPEAN JOURNAL OF PHYSICS

Eur. J. Phys. **22** (2001) 541–548 PII: S0143-0807(01)26039-5

Probing spatial variations in the index of refraction of air: a simple experiment using shadowgraph techniques

J M Modin, R M Batalha and R D Ramsier[1]

Department of Physics, University of Akron, Akron, OH 44325-4001, USA

E-mail: rex@uakron.edu

Received 22 June 2001, in final form 19 July 2001
Published 7 September 2001
Online at stacks.iop.org/EJP/22/541

Abstract

We describe a simple experimental arrangement for probing spatial variations in the index of refraction of air. Shadowgraph laser imaging techniques are used for the case of a horizontal cylinder heated to different temperatures which provides a highly symmetric and well defined geometry for demonstrating the usefulness of the shadowgraph approach. This experiment combines elements of geometrical and physical optics with concepts of thermal energy transfer and techniques for digital image analysis. The methodology can be adapted for the study of a wide range of optical media which exhibit variations in the index of refraction.

1. Introduction

Many studies are available which address the subject of energy transfer by natural convection from a heated cylinder. These usually address applications such as heat exchangers with the goal of understanding energy and mass transport under different physical situations. In this regard, finite difference techniques have been used for modelling systems in which the cylinder is housed in an unbounded fluid (i.e. the distance to the walls of the enclosure are much larger than the dimensions of the cylinder), and have addressed isothermal cylinders [1], cylinders with non-uniform surface temperatures [2], and entropy generation [3]. It is also clear that a simple experimental arrangement such as a heated cylinder can have educational value for undergraduate students trying to grasp the concepts of thermal energy transfer [4].

Optics is another area where simple experiments can be very revealing, and those involving how light travels through media with a varying index of refraction can be especially useful [5, 6]. Many optical techniques exist for imaging index variations, including laser speckle photography [7], wide angle scattering [8], laser pinhole and schlieren measurements [9] and shadowgraph methods [10, 11]. In the shadowgraph technique [12], a large diameter collimated

[1] Author to whom correspondence should be addressed.

laser beam is sent through a medium where the index of refraction varies in a direction perpendicular to that along which the light propagates. The resulting image formed on a distant screen exhibits areas of high and low light intensity (shadows) due to the inhomogeneous optical medium through which the light passed. Recent uses of this technique have been for the study of shock waves in flow systems [10, 11], where the density and thus index of refraction of air change abruptly over a very narrow spatial region. The present effort extends the use of shadowgraph techniques to the case of a heated cylinder to probe for gradual density variations in air in the presence of a temperature gradient. We combine both optics and thermal energy concepts in one experimental arrangement which can be easily adapted to a wide variety of physical systems.

2. Experimental method

The experiments are performed in a darkroom on a 76.2 cm $\times$ 152.4 cm optical breadboard (Melles Griot) complete with vibration isolation. Linearly polarized light is supplied by a Melles Griot TEM_{00} 5 mW linearly polarized He–Ne laser as illustrated in the top view portion (lower half) of figure 1. Since a large area needs to be illuminated uniformly, a combination spatial filter and beam expander/collimator from Oriel Instruments is used. The spatial filter is a 25 μm pinhole and the beam expander a 60$\times$ microscope objective. The final diameter of the collimated laser beam is approximately 46 mm. To adjust the intensity of the light falling on the charge coupled device (CCD) camera, a linearly polarizing filter is placed between the laser and the beam expander. A front surface mirror is incorporated to increase the optical path length, also illustrated from a top view in figure 1.

The heating element is a cylinder 15.8 mm in diameter (measured at room temperature) and 6.00 cm long with a power rating of 150 W at 120 V. A small screw is fastened with high-temperature JB Weld epoxy to the ceramic core of the heating element where the power leads emerge. After the epoxy hardens, an optical post is attached to the end of the screw. Temperature measurements of the surface of the heating element are made with a type K thermocouple spot-welded to the underside and very near the centre of the cylinder. This provides excellent thermal contact without obstructing the shadowgraph image. The heating element is then mounted on the breadboard and aligned with its axis parallel to the collimated laser beam. The cylinder mounting scheme is schematically represented in the exploded side view portion (upper half) of figure 1. It should be noted that since this drawing is strictly two-dimensional and not from perspective, cylindrical objects such as the heating element and post mount appear rectangular.

Data acquisition is accomplished with an EG&G Reticon MD4013 digital CCD camera with a resolution of 1024 $\times$ 1024 pixels on a 13.8 mm square chip, interfaced to a computer via a DIPIX XPG-1000 Power Grabber board. Since shadowgraph techniques are being used, the camera is set up with the CCD chip exposed directly to the beam at normal incidence. Because of the small size of the detector area, and to fit the entire image onto the CCD array, the shadowgraph of the heating element is reduced by a plano-convex lens with a focal length of 127.0 mm and a 76.2 mm aperture.

The heating element is powered by a 10 A, 120 V variable autotransformer and its surface temperature measured by a Fluke digital millivolt meter using a Fluke thermocouple converter. In order to achieve reproducible steady-state conditions, heating and cooling curves of the cylinder are collected for various power settings of the autotransformer. Figure 2 presents a representative data set indicating that steady-state conditions are reproducibly obtainable with the experimental set-up. It should be noted that logarithmic plots of the cooling curves indicate that this cooling is not strictly exponential in nature, consistent with the findings of Spuller and Cobb for vertical cylinders [4].

Prior to recording shadowgraphs, the camera is powered and allowed to stabilize. The image capture program displays images in real time on the computer monitor and updates about once per second. The software package supplied with the interface board saves the

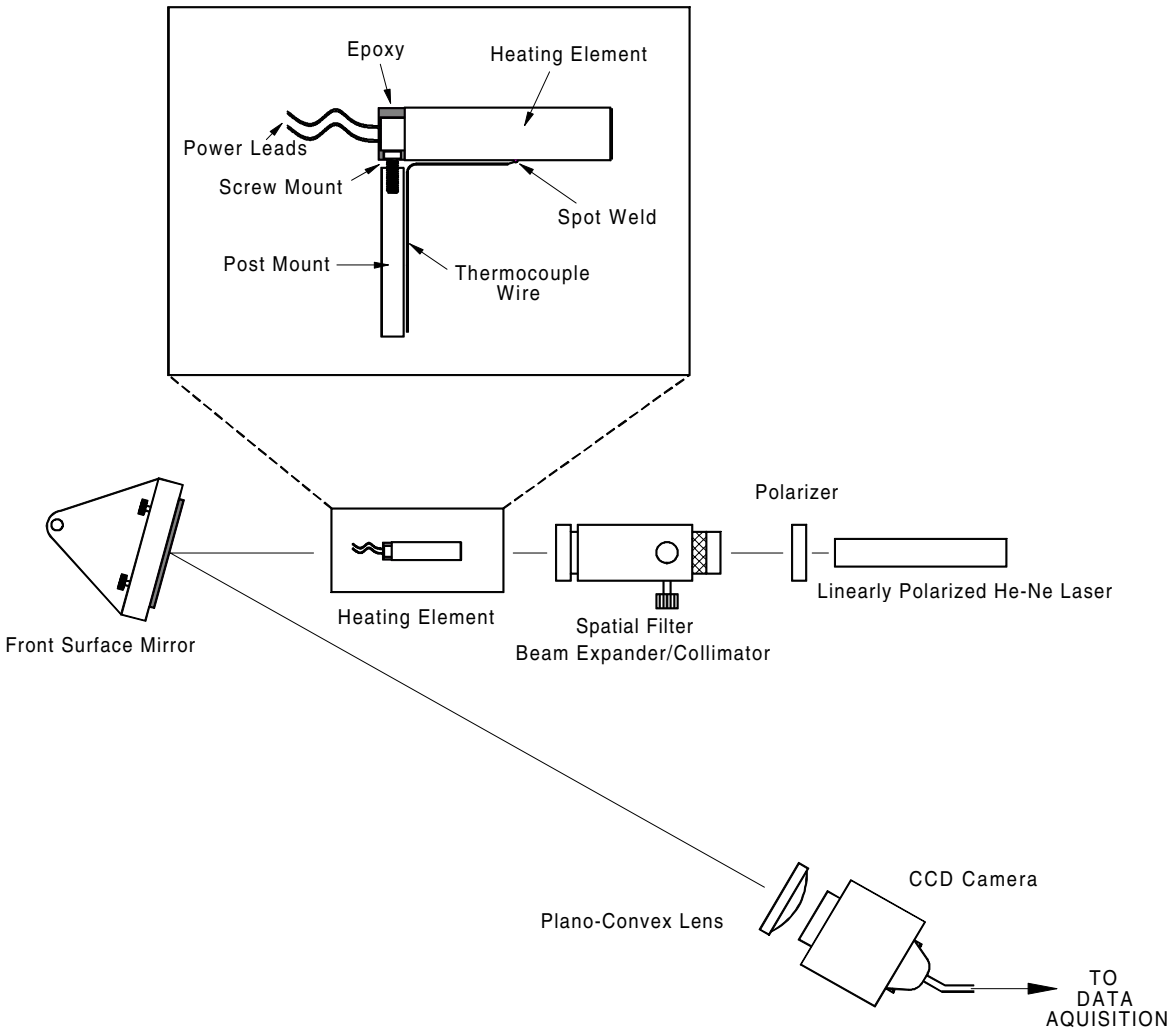

Figure 1. Schematic illustration of the experimental arrangement for shadowgraph imaging. The lower portion represents a top view of the entire apparatus, whereas the upper portion depicts an exploded side view of the heating element and its mounting. In this two-dimensional drawing, cylindrical objects (such as the heating element) appear rectangular.

captured images as 1 MB TIFF files. Before power to the heating element is applied, the room is darkened and the polarizer adjusted so that the intensity of the beam provides good image contrast without CCD saturation.

The autotransformer is adjusted in 10% power increments and, as can be seen in figure 2, it is sufficient to wait about 20 min to guarantee thermal equilibrium. At this time an image is captured while avoiding disturbing the air in the vicinity of the heating element. The images are viewed in PaintShop Pro and converted into data files containing a matrix of numbers representing the 8 bit pixel intensity and the pixel element's location in the image. The converted data are analysed in Sigma Plot and Excel to obtain one-dimensional line-cuts across the images.

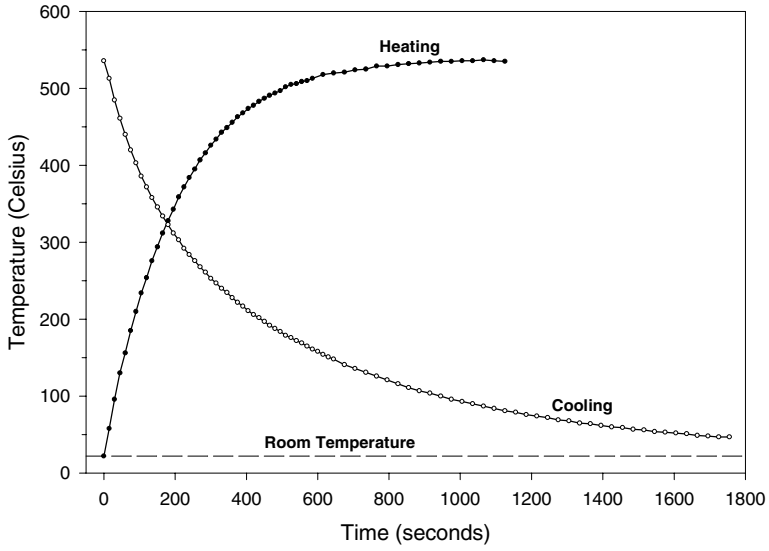

Figure 2. Representative heating and cooling curves of the cylinder.

3. Results and discussion

Figure 3 presents representative shadowgraph images of the cylinder at (A) 23 °C, (B) 280 °C and (C) 520 °C. The images clearly show the effects of diffraction from the lens and the heating element as well as plume formation above the cylinder as the temperature is increased. The aspect ratio (width/height) of the 'shadow' of the heating element increases with temperature, which can be attributed to variations in the density and therefore in the index of refraction of the air surrounding the cylinder. For a more quantitative analysis, figure 4 presents a series of horizontal line-cuts bisecting the shadowgraphs at eight different temperatures. Slight asymmetry of the intensities of the features (most obvious in the bottom curve of figure 4) are a result of variations of the CCD response across the array and slight misalignment of the array and heating element with respect to the optical axis. From data such as these, we can extract the pixel locations of the diffraction maxima due to the cylinder as a function of temperature. It is expected that, as the temperature is raised, the index of refraction of the air nearest the cylinder will decrease. Radially along a horizontal bisector there will be a positive gradient in the index of refraction making the region act as a diverging lens and causing the diffraction maxima to move outward as seen in figure 4.

We analyse the pixel locations of the first five diffraction maxima from the heating element for each of the line-cuts in figure 4. These data are shown in figure 5, and are presented as the average shift or displacement (in pixels) from the room-temperature location of each maximum as a function of temperature. The numerical average of the pixel locations of each maximum from the left-hand and right-hand sides of figure 4 is used in order to minimize effects of asymmetry as mentioned previously.

In the standard diverging lens model in geometrical optics (i.e. thin, double-concave lens), the angle of incidence with respect to the interface normal and the physical thickness of the optical medium increase as one moves away from the optical axis, but the index of refraction of the lens is assumed constant. In the present case, the physical thickness and angle of incidence is assumed constant and the data are used to probe the index of refraction profile versus radial distance from the cylinder as a function of its temperature. The experiment is designed to permit the use of far-field approximations, and we can calibrate our images based on the geometric shadow and measured diameter of the cylinder at room temperature (e.g.,

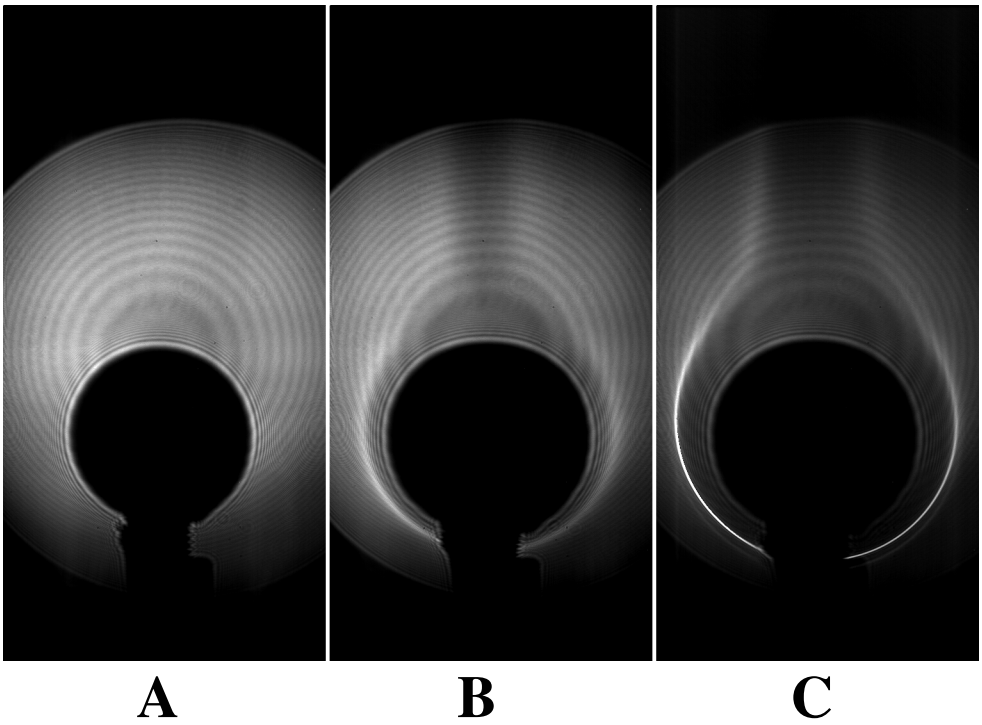

Figure 3. Representative shadowgraph images of the cylinder at (A) 23 °C, (B) 280 °C, and (C) 520 °C.

260 pixels = 15.8 mm).

Referring to figures 4 and 5, it is observed that the diffraction maxima shift with temperature at different rates and also that the displacement of each saturates. In a geometrical optics view, this is because the light involved in each maximum originates from the cylinder travelling a slightly different direction. The light producing the first maximum travels nearest to the optical axis of the system but at a slight angle with respect to the cylinder. As it travels in the forward direction past the cylinder it also travels outward, and in doing so encounters cooler regions of air with slightly higher indices of refraction. This in turn causes the light to refract farther from the symmetry axis and to suffer a larger total displacement by the time it reaches the detector.

The light forming the higher-order maxima experiences the same effect which becomes successively more pronounced with increasing order number since the original angle of deviation from the optical axis is larger. Thus this light encounters more regions of air across which the temperature varies as it travels to the detector, resulting in the higher-order maxima having the greatest overall displacement with cylinder temperature. The displacements shown in figure 5 can be thought of as the net sum or integrated effect of refraction from each of the regions of air that the light passes through. The effect saturates with the formation of a boundary layer of air which is seen in the data of figure 4 as a broad feature that becomes more well defined at higher temperatures.

In order to interpret these data, we need to consider what information is actually contained in the shadowgraph images. Following the discussion by Merzkirch [12], let us consider the measured displacements of the maxima (i.e. figure 5) as differences in the intensity (I) distributions recorded by the camera as a function of cylinder temperature. Letting T_0 be room temperature, and T the cylinder temperature during each shadowgraph measurement, it can be

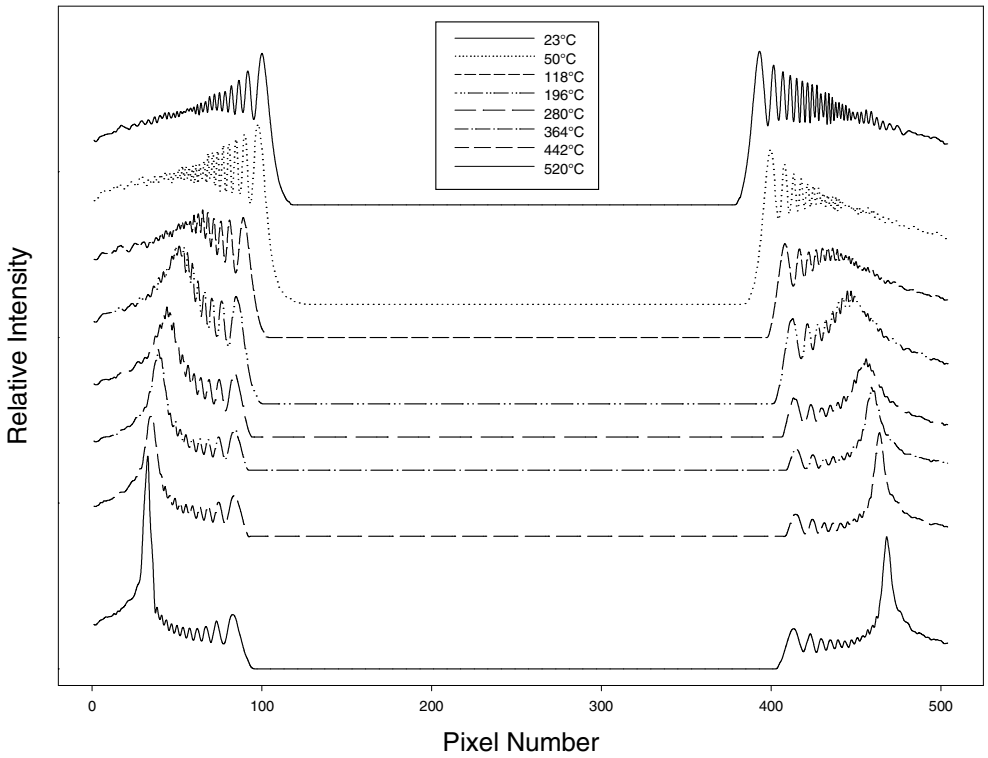

Figure 4. Cross-sectional line-cuts taken along horizontal bisectors of shadowgraph images of the cylinder at eight different temperatures.

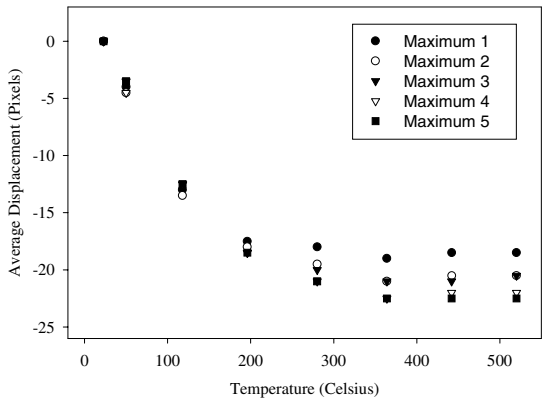

Figure 5. Average displacement of the first five diffraction maxima from their room temperature locations versus the surface temperature of the heating element.

shown that differences in the intensity distributions are related to the index of refraction (n) by

$$\Delta I = I(T) - I(T_0) \propto \int \frac{\partial^2}{\partial r^2}(\ln n)\,\mathrm{d}z \tag{1}$$

where r is the radial direction outward from the cylinder and z the forward direction along

the cylinder toward the detector. Equation (1) shows that shadowgraphs are sensitive to the curvature of the index of refraction profile in the inhomogeneous optical medium through which the light travels, in this case the air surrounding the heating element. If the curvature is zero, then each of the maxima would suffer the same displacement and the data points at each temperature in figure 5 would coincide. This would be equivalent to shining light through a wedge of glass; all the (monochromatic) rays would deflect by the same angle. Since this is not the case for the present situation, the curvature is certainly non-zero and most probably not constant.

Numerical solutions to the Navier–Stokes equations for the case of an isothermal horizontal cylinder demonstrate that the temperature of the air surrounding the heating element decreases with r [1], in a manner that is qualitatively similar to exponential decay. For the simple case of an ideal gas, we know that the mass density (ρ) is inversely proportional to the absolute temperature. Using the Gladstone–Dale relationship

$$(n - 1) = \kappa\rho \tag{2}$$

where $\kappa = 2.25 \times 10^{-4}$ m^3 kg^{-1} for air at the wavelength of the He–Ne laser [10], we would expect that the index of refraction is also inversely related to temperature. So as the temperature falls with increasing distance from the cylinder the index of refraction rises, which is consistent with the data presented herein. In actuality, the temperature dependence of the index of refraction of air is known empirically [13] and is more complicated than a simple inverse relationship. This is not surprising if one recalls that the ideal gas equation of state is simply the first term in a series expansion involving temperature-dependent virial coefficients.

Therefore, even if the temperature profile $T(r)$ followed a simple functional dependence (which it does not as evidenced by our inability to accurately fit the data presented in [1] with simple functions), the density and thus index of refraction profile $n(r)$ will contain higher-order terms which result in a non-zero curvature. We therefore expect the resulting shadowgraph images to exhibit non-uniform displacements for rays travelling in different directions, consistent with the observations reported in this work. Quantitative determination of $n(r)$ from the shadowgraph images would involve a double integration of the measured intensity distributions such as those in figure 4. This could result in large uncertainties because of the finite number of raw data points and is a procedure that is usually unnecessary for most practical purposes. However, the simplicity of the shadowgraph method makes it a convenient tool for quickly detecting variations in the optical density of various media, and in the case discussed here we demonstrate its use for combining thermodynamics and optics concepts into one laboratory exercise.

4. Conclusions

We present a simple experiment which can be used to help students learn about the thermal and optical properties of air within a conceptual framework. The apparatus and methodology can be easily adapted to a variety of inhomogeneous media, but the heated cylinder is a well defined system to demonstrate in principle the use of shadowgraphs in the undergraduate laboratory. The richness of the physics of thermal energy transfer and mass transport is obvious in the resulting data, and we discuss various aspects of the problem. Digital image analysis plays a major role in the shadowgraph technique and is a skill that students can master within the context of laboratory activities like the one described here.

Acknowledgments

The authors are grateful to Professor S I Hariharan for helpful ideas and access to the CCD camera, and to Professors P N Henriksen and N Ida for their advice on various aspects of this work.

References

[1] Kuehn T H and Goldstein R J 1980 Numerical solution to the Navier–Stokes equations for laminar natural convection about a horizontal isothermal circular cylinder *Int. J. Heat Mass Transfer* **23** 971
[2] Farouk B and Güçeri S I 1981 Natural convection from a horizontal cylinder—laminar regime *ASME Trans. J. Heat Transfer* **103** 522
[3] Abu-Hijleh B A/K, Abu-Qudais M and Abu Nada E 1999 Numerical prediction of entropy generation due to natural convection from a horizontal cylinder *Energy* **24** 327
[4] Spuller J E and Cobb R W 1993 Cooling of a vertical cylinder by natural convection: an undergraduate experiment *Am. J. Phys.* **61** 568
[5] Krueger D A 1980 Spatially varying index of refraction: an open ended undergraduate topic *Am. J. Phys.* **48** 183
[6] Mamola K C, Mueller W F and Regittko B J 1992 Light rays in gradient index media: a laboratory exercise *Am. J. Phys.* **60** 527
[7] Guo Z-Y, Song Y-Z and Lin Z-X 1995 Laser speckle photography in heat transfer studies *Exp. Thermal Fluid Sci.* **10** 1
[8] Panda J 1995 Wide angle light scattering in shock–laser interaction *AIAA J.* **33** 2429
[9] Panda J 1995 Shock detection technique based on light scattering by shock *AIAA J.* **33** 2431
[10] Panda J and Adamovsky G 1995 Laser light scattering by shock waves *Phys. Fluids* **7** 2271
[11] Hariharan S I and Johnson D K 1995 Transmission of light waves through normal shocks *Appl. Opt.* **34** 7752
[12] Merzkirch W 1987 *Flow Visualization* 2nd edn (Orlando, FL: Academic) pp 115–34
[13] 1994 *CRC Handbook of Chemistry and Physics* 75th edn (Boca Raton, FL: CRC Press) p 10-302